Thermal-Degradation Characteristics of Mechanically Nanofibrillated Bleached Pulps from Hardwood and Softwood

Akihiro Hideno *

Nanofibrillated cellulose (NFC) consists of ultrafine cellulose structures in which the fibrils can have widths in the range from about 5 to 100 nm. NFC has been studied and developed in the paper industry, using bleached pulp from wood as the raw material. One of the issues in the application of NFC is their heat resistance to thermal degradation. The production process of NFC results in a decrease in their pyrolysis temperature during the nanofibrillation of bleached pulp; however, the details behind the reason and mechanisms are still unclear. In this study, NFC was prepared from bleached hardwood and softwood pulp by mechanical nanofibrillation using a grinder, and the pyrolysis behavior was investigated. For both bleached pulps, a decrease in the pyrolysis temperature was observed after nanofibrillation. The results suggest that the decrease in the pyrolysis temperature from nanofibrillation is not due to damage of the crystalline cellulose by nano fibrillation, but the damage of the hemicellulose components in the surface of the cellulose microfibrils or the interface between the crystalline cellulose and hemicellulose. If the hemicellulose on the surface of crystalline cellulose could be removed from the NFC, then the decrease in the pyrolysis temperature could be suppressed.

DOI: 10.15376/biores.18.4.8573-8584

Keywords: Mechanical nano fibrillation; Bleached pulp; Thermogravimetric analysis; DTG peak separation; Damaged hemicellulose

Contact information: Paper Industry Innovation Center, Ehime University, 127 Mendori-cho, Shikokuchuo, Ehime 799-0113, Japan Tel: +81-089-622-3230;
** Corresponding author: a-hideno@agr.ehime-u.ac.jp*

INTRODUCTION

Cellulose nanofibers (NFC), which can be prepared from plant fibers such as wood pulp, wastepaper, and citrus juice residue, have high functionality such as light weight, high strength, high transparency, and high specific surface area. Consequently, research institutes and companies in Japan and abroad are developing a wide range of applications such as automobile components, home appliance housings, and cosmetic materials (Yano 2010; Isogai *et al*. 2011).

One of the major issues in the development of NFC applications is the improvement of thermal stability. By mixing NFC with resin, it is possible to achieve lighter weight and higher strength and to replace fossil resource-derived materials with natural fibers. However, resin kneading is usually performed at approximately 140 to 250 °C. The coloration and damage to the NFC caused during kneading with plastics (polyethylene, polypropylene, and polyamides, *etc*.) are considered problematic above 200 °C in general

(Semba *et al*. 2021). Coloration during drying is also a problem when NFC sheets or thin sheets are produced.

NFC production requires fiber disassembly down to the nanoscale, which damages fibers during nanofibrillation. As cellulose is defibrillated and nanofibrillated, its pyrolysis temperature decreases, and coloration and pyrolysis occur at relatively low temperatures. Microfibrillation of cellulose significantly reduces thermal stability (Quievy *et al*. 2010); it is imaginable that the thermal stability of NFC that is further defibrillated than microfibrillated cellulose is generally lower. However, limited systematic and detailed analysis has been conducted on the pyrolysis of NFC. This topic has recently been the focus of active research and development, and there have been limited examples of research aimed at making NFC more heat resistant.

Saka and Kawamoto *et al*. showed that the loss of the reducing end of microcrystalline cellulose powder (Avicel) significantly stabilizes it against thermal decomposition at approximately 200 to 280 °C, suggesting that the thermal decomposition of the reducing end has a significant impact on the dehydration, coloration, and carbonization of cellulose (*e.g.*, Kawamoto 2015). They proposed a mechanism whereby the pyrolysis of cellulose is activated by pyrolysis at the microcrystalline interface, including pyrolysis at the reducing end and in the amorphous region. They also examined differences in the pyrolysis behavior of hemicellulose and cellulose in the cell walls of hardwood and softwood and found that isolated xylan containing uronic acid residues could act as a catalyst for pyrolysis and is more reactive than isolated glucomannan; however, xylan in wood has a significantly higher thermal stability and is in the same pyrolysis temperature range as glucomannan in wood (Wang *et al*. 2020). Cellulose in softwood is bound to and covered by glucomannan, whereas xylan and lignin are thought to exist between the glucomannan and glucomannan bound to cellulose. Xylan in hardwood has been shown to be strongly bound to cellulose. The cited authors further investigated the pyrolysis behavior of hemicellulose and cellulose in ball-milled softwood and hardwood and found that the pyrolysis reactivity of cellulose and hemicellulose was significantly different between softwood (cedar) and hardwood (beech). Uronic acids and their salts act as acid and base catalysts, respectively, and their specific arrangement in the cell wall is thought to be a factor influencing the degradation reactivity (Wang *et al*. 2021a). The effect of lignin on pyrolysis has also been investigated by delignifying softwood and hardwood by the Wise oxidation method and examining the pyrolysis behavior of holocellulose. As a result, similar TG/DTG profiles were reported for holocellulose from softwood cedar and hardwood beech with the lignin removed (Wang *et al*. 2021b).

There have been research reports on the pyrolysis behavior of softwood and hardwood, holocellulose after delignification, and isolated components. There have been reports on the pyrolysis behavior of bleached kraft pulps, which are currently the mainstream in paper manufacturing; however, there are few examples of detailed analysis. These bleached pulps, obtained from wood chips after kraft pulping and multistage bleaching, are also the main raw material for NFC because they can be supplied in large quantities at a low cost. These bleached pulps contain cellulose and partially degraded hemicellulose. The pyrolysis temperature of bleached kraft pulp is affected by mechanical defibering during NFC preparation; however, little is known about it.

In a previous study (Hideno 2016), ball milling crystalline cellulose resulted in a significant reduction in crystallinity while there was only a slight decrease in the pyrolysis temperature. The authors reported that the ball milling treatment of wood flour not only damaged the crystalline cellulose but also damaged the hemicellulose, since not only the

degree of crystallinity but also the pyrolysis temperature was significantly reduced.

Although useful knowledge has been accumulated on the pyrolysis of cellulose, there is a lack of knowledge on the pyrolysis of NFC. In this study, bleached hardwood and softwood pulp were selected as representative raw materials for NFC. Subsequently, NFC was prepared by mechanical defibrillation followed by detailed thermal analysis as well as quantification and comparison of apparent crystallinity and reducing ends. The degree of influence of the mechanical fiber breakage treatment on the pyrolysis temperature of wood pulp varied with the type of pulp, suggesting that the original composition and apparent crystallinity contributed significantly to the pyrolysis temperature of wood pulp.

In this study, the effects of mechanical nano fibrillation and the different types of pulp on the thermal degradation properties of bleached wood pulp were investigated and compared. Two types of pulp (bleached pulp from softwood and hardwood) were selected, mechanically nanofibrillated, and analyzed by thermal analysis in detail.

EXPERIMENTAL

Materials

Bleached kraft pulp from hardwood and softwood, that are referred to as Loubholtz Bleached Kraft Pulp (LBKP) and Nadleholz Bleached Kraft Pulp (NBKP) respectively, were purchased from HONDA YOKO Co., LTD in Japan. The two kinds of pulp were refined by Valley beater to approximately the Canadian standard freeness of 100 based on the ISO 5264-1 method.

Mechanical Nano Fibrillation

Refined pulp slurry (solid content 2 wt%) of 1 kg was mechanically nano fibrillated by a grinder (Super Masukoroider, MKCA6-2, Masuko Industry Co., Japan) for approximately 60 min based on previous reports (Abe and Yano 2009; Hideno *et al*. 2009). The obtained NFC were pasteurized at 80 °C for more than 30 min and stored at 4 °C.

Measurement of Constituent Sugars in Pulp

The constituent sugars in the pulp (NBKP and LBKP) samples were analyzed using a modified National renewable energy laboratory (NREL) method (Sluiter *et al*. 2008). Approximately 30 to 50 mg of the dried sample and 0.3 mL of 72% sulfuric acid were mixed in a 2- mL tube with a vortex. The pulp sample was dissolved in the 72% sulfuric acid by crushing with a glass rod at 10 to 15 min intervals while stirring at 30 °C for 60 min using a tube rotator. This hydrolyzed sample was transferred into a glass tube with a cap, diluted with 8.4 mL of pure water, and autoclaved at 121 °C for 60 min. This twice-hydrolyzed sample was cooled to under 30 °C and filtered using a glass filter. The filtrate was transferred to a measuring flask, adjusted up to 20 mL with pure water, and neutralized by barium sulfate solution, and the monomeric sugars in it were measured using the HPLC system (JASCO Engineering Co., Japan) equipped with a CarboSep CHO-782 column (300 mm× 7.8 mm, 7-μm particle size, CONCISE SEPARATIONS Co., USA) and a refractive index (RI) detector. The effluent rate of the HPLC-grade pure water was 1 mL min^{-1} and the column oven was set up at 80 °C.

Morphological Observation by Electron Microscope of Pulp and NFC

The pulp fibers and NFC samples were diluted with ethanol as appropriate, solvent-exchanged with a tertiary butyl alcohol, and freeze dried. The dried samples were adhered to conductive seals, coated with osmium tetroxide by an osmium coater (HPC-1SW, VACUUM DEVICE Co., Japan), and observed by field-emission scanning electron microscopy (JSM-7610FF, JEOL Co., Japan) at an acceleration voltage of 1.5 to 5 kV.

Thermal Gravimetric Analysis (TGA)

The thermal gravimetric analyses (TGA) of the original pulps and prepared NFC were conducted as described in a previous report (Hideno 2016). Each freeze-dry sample (approximately 5 mg) was formed into a tablet (Φ 4.5 mm) with a hand press. A TGA instrument (TG/DTA6200, Seiko Instruments Inc., Chiba, Japan) was used under a nitrogen atmosphere at a flow rate of 100 mL min^{-1}. The measurement conditions were as follows: approximately 25 to 110 °C (40 °C min^{-1}), 110 °C for 10 min, 110 to 550 °C (10 °C min^{-1}), and 550 °C for 10 min. Differential thermogravimetric (DTG) and relative DTG curves were calculated using Eqs. 1, 2, and 3.

$$\text{TG (\%)} = (\text{weight loss due to thermal decomposition / original weight}) \times 100 \quad (1)$$

$$\text{DTG (\%/min)} = \text{TG (\%)} / \text{time for increase in temperature (min)} \quad (2)$$

$$\text{Relative DTG} = \text{DTG value} / \text{maximum DTG value (DTG curve peak)} \quad (3)$$

The sample weight at 110 °C was defined as the 100% dry weight. Curve-fitting for the DTG peak separation was conducted using the TA7000 version 10.41 (Hitachi High-Tech Science Co., Tokyo, Japan) and Fityk version 0.9.4 (Fityk, Warsaw, Poland). A split Gaussian method and a Levenberg-Marquardt algorithm were used for peak separation and DTG curve fitting, respectively.

X-ray Diffraction Analysis (XRD)

X-ray diffraction analysis was carried out as reported (Hideno *et al*. 2016), using an XRD instrument (Ultima IV, Rigaku Co., Japan) with CuKα radiation at 40 kV and 30 mA. The scan range and rate were 5 to 40° in 2θ and 1° min^{-1}, respectively. The crystallinity index (CrI) was calculated using the method presented by Segal *et al*. (1959), as shown in Eq. 4. The height of the 200 peak (I_{200}, 2θ = 22.5°) and the minimum between the 200 and 110 peaks (I_{am}, 2θ = 18.7°) were applied,

$$\text{Crystallinity Index (\%)} = [(I_{200}-I_{am})/I_{200}] \times 100 \quad (4)$$

where I_{200} represents the peak intensity of the crystalline cellulose I, and I_{am} represents the intensity of the amorphous fraction.

RESULTS AND DISCUSSION

Monomeric Constituent Sugars

Although many analyses have been published on the constituent sugars of hardwood and softwood lumber, relatively little data on the constituent sugars of bleached pulp has been obtained from them. In addition, since the composition of the pulp obtained varies depending on the digestion (kraft pulping) and bleaching methods, it is desirable to analyze the pulp used in research on a lot-by-lot basis. The contents of the constituent

monomeric sugars of LBKP and NBKP used in this study are listed in Table 1. Although glucose derived mainly from cellulose was higher in NBKP than in LBKP, there was no significant difference in the cellulose content because softwood lumber contains glucose as glucomannan. Xylose derived from xylan of LBKP clearly had a higher content than that of NBKP. Glucomannan-derived mannose was not detected in LBKP, but only in NBKP. Because softwoods originally contained more mannose than hardwoods, and hardwoods contained only trace amounts of mannose, it is inferred that no detectable mannose remained in LBKP after kraft pulping and multi-stage bleaching.

Table 1. Monomeric Constituent Sugars in Bleached Pulp of Hardwood and Softwood

Sample	Main Constituent Sugar (mg g^{-1})				
	Glucose	Xylose	Galactose	Arabinose	Mannose
LBKP	844.9±11.7	177.5±3.8	9.8±7.4	4.9±1.6	N.D.
NBKP	953.7± 8.4	94.3±2.3	28.9±2.5	11.0±1.9	57.3±6.9

Morphological Observation by Electron Microscope of Pulp and NFC

The pulp fibers of LBKP and NBKP were mechanically ground by the grinder. The FE-SEM images of LBKP, NBKP, and their NFC are shown in Fig. 1. Tightly bonded and accumulated cellulose microfibrils and their bundles were observed on the surface of the secondary cell wall in LBKP (Fig. 1 (a) and (b)) and NBKP (Fig. 1 (d) and (e)). After the mechanical nano fibrillation of LBKP and NBKP, NFC and their networks were observed (Fig. 1 (c) and (f)). Approximately 10 to 20 μm in width of pulp was subjected to approximately 20 to 50 nm in width by nano fibrillation.

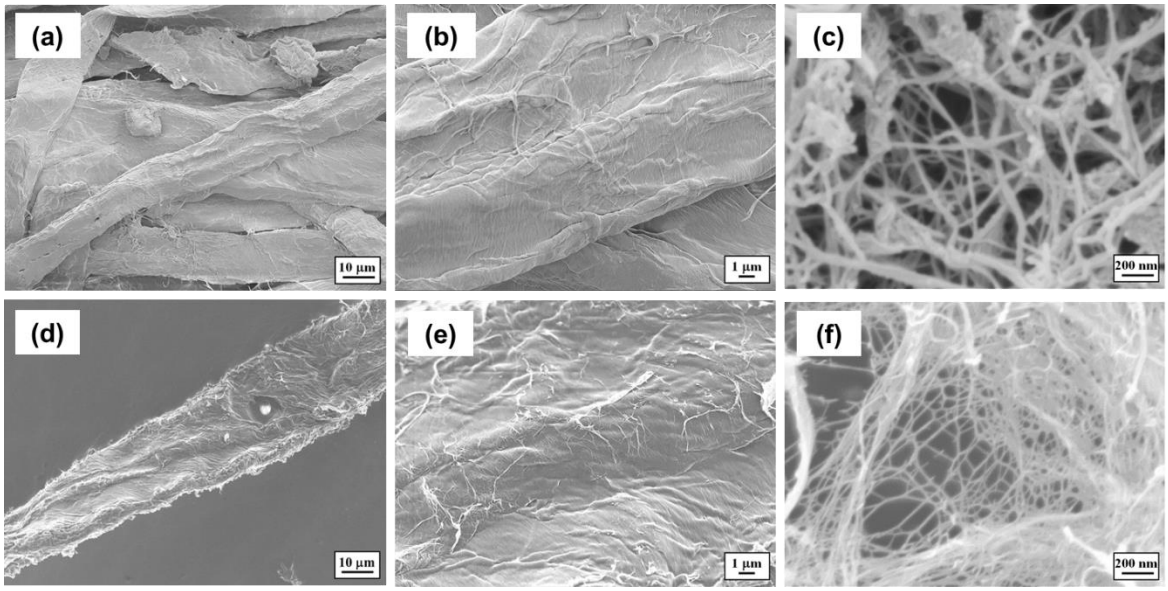

Fig. 1. Field-emission type scanning electron micrographs of LBKP ((a) and (b)), NBKP((d) and (e)), and their nano fibrillated samples ((c) and (f)), respectively

Thermal Gravimetric Analysis (TGA) of Pulp and NFC Samples

The thermal degradation temperature of NBKP was higher than that of LBKP, and the trend was the same after mechanical nanofibrillation (Fig. 2). Both LBKP and NBKP decreased in the pyrolysis temperature by nanofibrillation; however, LBKP exhibited a larger decrease in the pyrolysis start temperature than NBKP (280.9 to 267.7 °C in LBKP *vs*. 284.0 to 274.1 °C in NBKP at 5% weight loss). Comparing the difference in the pyrolysis temperatures between the original bleached pulps and NFC, the difference between the LBKP and LBKP-NFC was larger in the early stages of pyrolysis, whereas the difference between NBKP and NBKP-NFC increased after the middle stage of pyrolysis; however, the temperature difference between LBKP and LBKP-NFC was larger than that between NBKP and NBKP-NFC (Table 2). Therefore, LBKP was found to be more susceptible to mechanical nano fibrillation than NBKP, and the nano fibrillation may have formed more substances on its surface that pyrolyze on the low temperature side. According to previous studies, a shoulder peak was identified in the DTG peaks of hardwoods before the main peak (Wang *et al*. 2020), but it was hardly visible in the DTG curve of LBKP in this study. A slight shoulder peak was observed in the DTG peak of NFC prepared from LBKP. Therefore, DTG peaks obtained from the thermal analysis of each NFC sample were separated and compared.

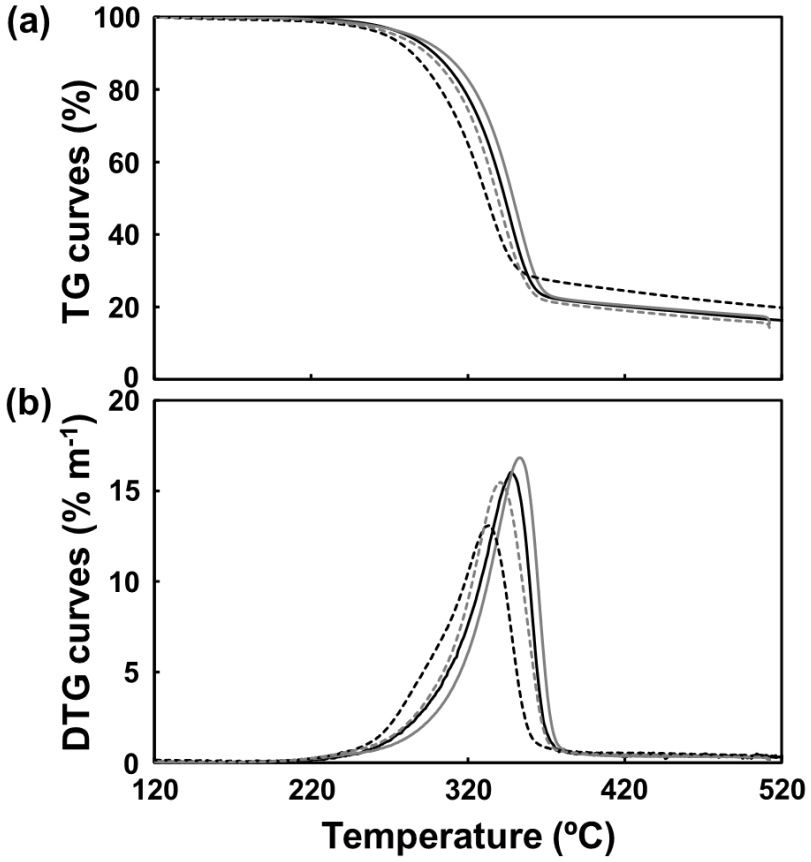

Fig. 2. Thermal gravimetric (TG) (a) and derivative thermogravimetric (DTG) (b) curves of LBKP (black solid lines), nano fibrillated LBKP (black broken lines), NBKP (gray solid lines), and nano fibrillated NBKP (gray broken lines)

Table 2. Thermal Degradation Temperatures of Original Pulps and NFC at 1, 5, and 10% Weight Loss and DTG peaks

	Temperature at Weight Loss (°C)			DTG Peak (°C)
Sample	1%	5%	10%	
LBKP	239.8	280.9	298.4	347.4
LBKP NFC	207.8	267.7	284.5	333.3
NBKP	232.0	284.0	304.3	353.0
NBKP NFC	226.7	274.1	293.8	340.5

Comparison of Separated DTG Peaks of Pulp and NFC Samples

The peak separation of the DTG curves obtained from the pyrolysis of each NFC resulted in four separate DTG peaks; the DTG peak separation revealed traces of the LBKP shoulder peak (Fig. 3 (a) black dotted line indicated by a black arrow), which could not be identified before the separation. The shoulder peak became apparent after nanofibrillation and was also confirmed (Fig. 3 (b) the region of the solid line indicated by a white arrow) by the original DTG peak (before separation). The DTG peak of the NBKP derived from softwood wood did not originally have a shoulder peak. The second peak of DTG separation was also close to the pyrolysis of cellulose on the high temperature side, and no trace of the shoulder peak was observed (Fig. 3 (c)). The comparison of the major first and second separation peaks among the DTG separation peaks is shown in Fig. 4. The analysis of the separation peaks suggests that the lower pyrolysis temperatures of crystalline cellulose (NBKP and LBKP) and amorphous cellulose or hemicellulose (NBKP) are the main reasons for the lower pyrolysis temperatures in the nanofibrillation. It was reported that cellulose and hemicellulose degradation occurred simultaneously in cedar (softwood), whereas cellulose and hemicellulose pyrolyzed independently in beech (hardwood), with the shoulder peak of the DTG curve being identified by the pyrolysis of the hemicellulose (Wang *et al*., 2020). Cellulose degradation began at approximately 260 °C, at which point approximately half of the xylan and part of the glucomannan was degraded, followed by rapid degradation of the remaining hemicellulose at approximately 300 to 320 °C, and then rapid degradation of the cellulose at 320 to 340 °C. Unlike beech holocellulose in hardwood lumber, the authors consider that the cellulose degradation of cedar holocellulose is closely related to the degradation of hemicellulose. The results of the above previous studies show a similar trend in the results of the separated DTG peaks in this study. However, they reported that the TG/DTG profiles of the cedar and beech wood samples were different but similar for holocellulose when lignin was removed (Wang *et al*. 2021b); the results of this study showed that the pyrolysis temperature of LBKP from hardwood wood was lower than that of NBKP from softwood wood. Moreover, mechanical nano fibrillation increased the difference in the pyrolysis behavior between LBKP NFC and NBKP NFC, and a shoulder peak of the DTG curve was observed in LBKP NFC.

Both the first and second major peaks of the separated DTG curves were higher for NBKP than for LBKP. The difference in the second major peak was particularly large. Based on previous studies (Hideno 2016), it is likely that the first separation peak represents pyrolysis of crystalline cellulose, whereas the second major peak represents pyrolysis of the amorphous components. This was likely due to the significant difference

in hemicellulose between LBKP and NBKP. The crystalline cellulose and hemicellulose in NBKP had higher pyrolysis temperatures and higher binding strength to each other than those in LBKP. Particularly, the differences of the binding style between cellulose and hemicellulose, and among hemicellulose would affect their thermal degradation properties.

Comparing the difference in the thermal-degradation temperatures before and after nano fibrillation for the first and second separation peaks, the difference before and after nano fibrillation decreased as the percentage of thermal-degradation weight loss increased for both peaks. This means that the effect of mechanical nanofibrillation was greater in the early stages of thermal degradation, suggesting that the damage to materials in the lower thermal-degradation temperature range was greater. In the first separation DTG peak, a comparison of the difference in pyrolysis temperatures before and after nano fibrillation showed that the pyrolysis temperature of LBKP with 10% weight loss decreased by 72.2 °C owing to nano fibrillation, whereas that of NBKP decreased by 17.6 °C. The second separation DTG peak also decreased by 42.9 and 19.5 °C, respectively. Their results suggest that the materials (amorphous cellulose and hemicellulose) that undergo thermal degradation in the lower temperature region of LBKP were strongly affected by mechanical nano fibrillation.

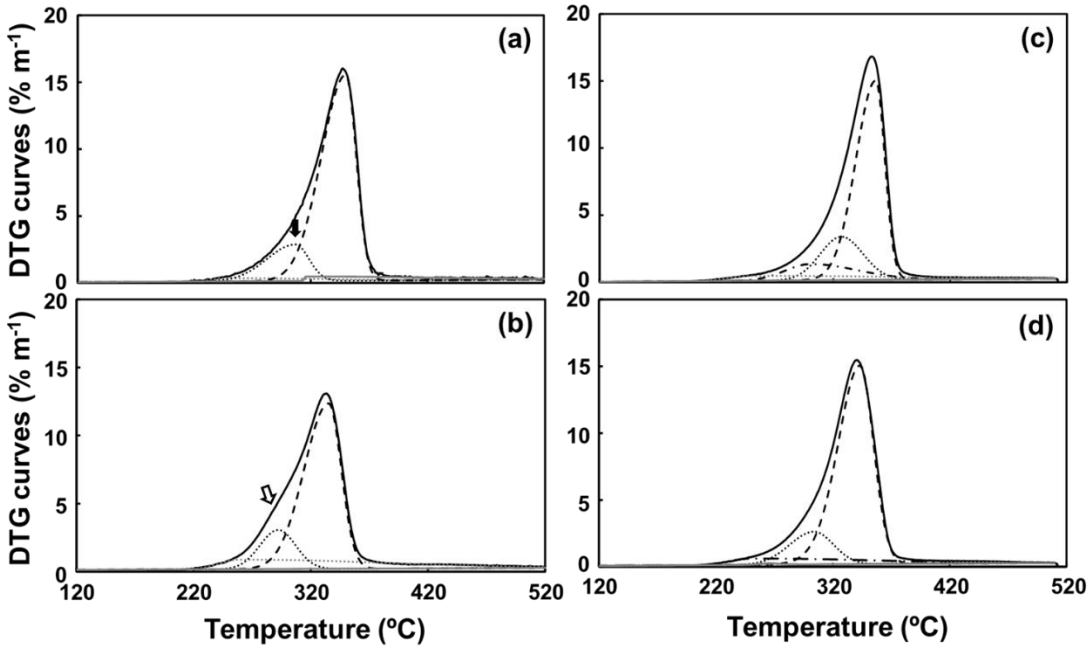

Fig. 3. Derivative thermal gravimetric (DTG) curves (solid lines) and separated and curve-fitted DTG curves (broken, dotted, and dashed and dotted lines) of (a) LBKP, (b) nano fibrillated LBKP, (c) NBKP, and (d) nano fibrillated NBKP. The black broken lines and dotted lines mean the main and sub separated peaks, respectively.

The major hemicellulose in hardwoods is arabinoxylan, whereas the hemicellulose in softwoods is glucomannan, and the results of the constituent sugar analysis are consistent (Table 1). The differences in the separation peaks obtained from thermal analysis may reflect differences in the strength of the chemical bonds between hemicellulose and cellulose. In other words, glucomannan, the major hemicellulose of conifers, may be more strongly bound to crystalline cellulose. Cellulose fibers in softwood are strongly bound to glucomannan and that the surface is covered (Kumagai and Endo 2018; Wang *et al*. 2020), which is consistent with the observations derived from the thermal analysis in this study.

Apparent Crystallinity Calculated from X-ray Diffraction Analysis

The XRD results in Fig. 4 showed that the nanofibrillation resulted in only a small decrease in apparent crystallinity and no significant difference in the multiple comparison method (Tukey method). The author's previous study showed that ball milling of microcrystalline cellulose resulted in a significant decrease in crystallinity but only a slight decrease in the pyrolysis temperature, whereas ball milling of wood powder resulted in a significant decrease in the pyrolysis temperature (Hideno 2016). Therefore, it is likely that the decrease in the pyrolysis temperature due to mechanical nanofibrillation is not primarily due to damage to the crystalline cellulose, but due to the damage to amorphous components (amorphous cellulose and hemicellulose).

According to Wang *et al*. (2020, 2021a,b) the reactivity of cellulose surface molecules plays a significant role in the thermal degradation of cellulose, and they expect the matrix and its degradation to affect the reactivity of cellulose microfibrils by affecting the surface cellulose microfibrils at the interface. From their report and the present results, it is considered that the mechanical nano fibrillation accelerates the decrease in the pyrolysis temperature by damaging xylan near the cellulose microfibrils in LBKP and glucomannan and xylan in NBKP, respectively, through the nanofibrillation.

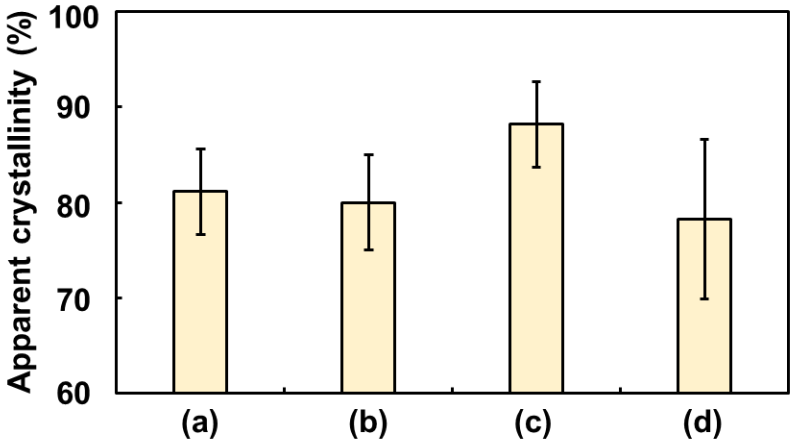

Fig. 4. Apparent crystallinity of (a) LBKP, (b) LBKP NFC, (c) NBKP, and (d) NBKP NFC

Schematic diagrams of the structure of the mechanical nanofibrillated bleached pulps based on previous studies and the present results are presented in Fig. 5. In hardwood, a matrix complex of xylan and lignin is halfway independent of the crystalline cellulose microfibrils (Wang *et al*. 2020). In softwood, glucomannan is present on the surface of the crystalline cellulose microfibrils and the xylan and lignin complexes are present as the matrix. Kraft pulping and multistage bleaching remove most of the lignin and hemicellulose, but some of the hemicellulose remains in the pulp as degradation products of hemicellulose and modified hemicellulose (Table 1). In other words, in LBKP derived from hardwoods, denatured or partially degraded xylan is loosely bound to the surface layer of the crystalline cellulose microfibrils. In NBKP from softwoods, denatured or partially degraded glucomannan is strongly bound to the surface layer of the crystalline cellulose microfibrils, and partially degraded xylan is present with the glucomannan. The mechanical nanofibrillation of LBKP and NBKP mainly damages the denatured or partially degraded hemicellulose on the surface layer. That is, the modified xylan of LBKP and the modified xylan and glucomannan of NBKP undergo physical destruction. The hemicellulose

component, which is originally more susceptible to thermal decomposition than crystalline cellulose, becomes even more susceptible to thermal decomposition under the influence of mechanical nanofibrillation and becomes the starting point for thermal decomposition. Xylan, which existed as halfway independent of crystalline cellulose in hardwood, remained as damaged modified xylan in LBKP-NFC, and is considered to have manifested as the shoulder peak of the DTG curve during pyrolysis. In NBKP-NFC, although the pyrolysis temperature was lower than in NBKP, the shoulder peak of DTG did not appear and the pyrolysis temperature was higher than that in LBKP-NFC because the crystalline cellulose microfibrils and modified glucomannan were strongly bound and the amount of damaged modified xylan was relatively small in LBKP-NFC and NBKP-NFC; the physically damaged modified xylan is likely the starting point for pyrolysis, and if it could be removed, the pyrolysis temperature could be increased.

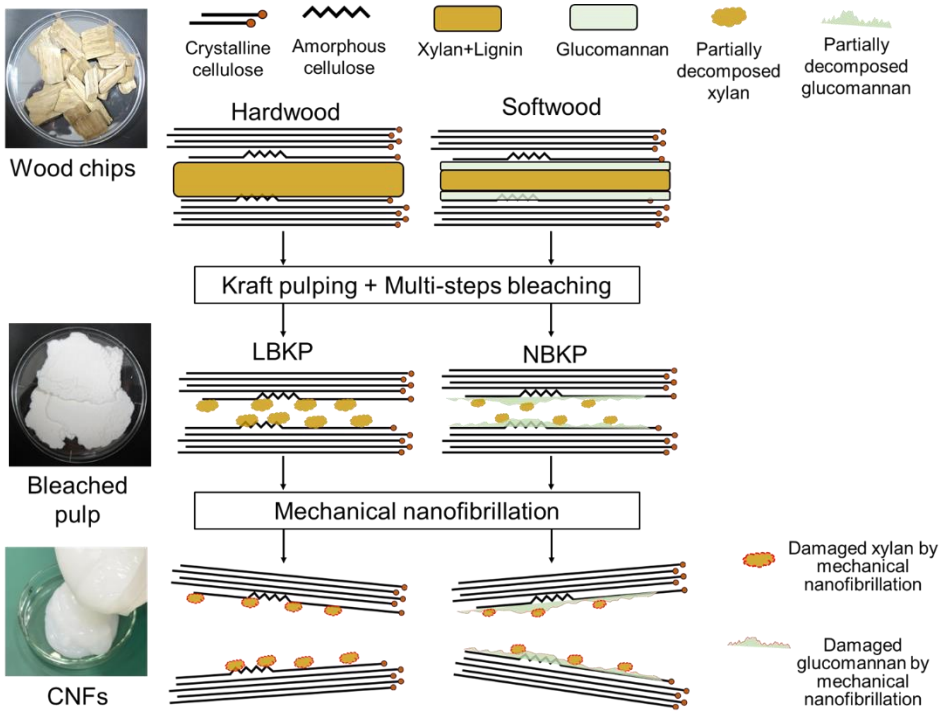

Fig. 5. Schematic diagram of structure of mechanical nano fibrillated bleached pulps from hardwood and softwood

CONCLUSIONS

The effects of mechanical nano fibrillation on the pyrolysis of bleached wood pulps (softwood=NBKP and hardwood=LBKP) were obtained through detailed thermal analyses (TG/DTG analysis, and curve fitting and peak separation of DTG curves) and crystallinity analysis. The conclusion is summarized as follows:

1. NBKP had a higher thermal-degradation temperature than LBKP, even after NFC preparation by mechanical nano fibrillation.
2. Nanofibrillation significantly reduced the pyrolysis temperatures of both pulps.

3. For the differential thermogravimetric (DTG) curve of LBKP, the shoulder peak reported for hardwood lumber could not be confirmed. However, when the DTG curve was peak-separated, an internalized shoulder peak was confirmed. Furthermore, the shoulder peak of the DTG curve became apparent in LBKP-NFC after nanofibrillation.
4. Peak separation analysis of the DTG curves revealed that the pyrolysis temperatures of both pulps were greatly reduced because the pyrolysis was originally accelerated in the low-temperature region by nanofibrillation.
5. The crystallinities of cellulose were hardly changed by nano fibrillation in LBKP and NBKP.
6. The decrease in the pyrolysis temperature due to nano fibrillation of bleached wood pulp is most likely due to damage to the hemicellulose present in the crystalline cellulose surface layer, rather than damage to the crystalline cellulose.

ACKNOWLEDGMENTS

The author thanks the Advanced Research Support Center of Ehime University for leasing TGA instruments, and the Ehime Institute of Industrial Technology for leasing the FE-SEM and XRD instruments. The author would also like to thank Prof. Hiroyuki Yano, Prof. Haruo Kawamoto (Kyoto University, Uji, Japan), and Prof. Kenichiro Tanoue (Yamaguchi University, Ube, Japan) for their valuable comments. This work was supported by JSPS KAKENHI (Grant No. JP16K07809, 20K06345, and 23K05491).

REFERENCES CITED

Abe, K., and Yano, H. (2009). "Comparison of the characterization of cellulose microfibril aggregates of wood, rice straw and potato tuber," *Cellulose* 16, 1017-1023. DOI: 10.1007/s10570-009-9334-9

Hideno, A., Inoue, H., Tsukahara, K., Fujimoto, S., Minowa, T., Inoue, S., Endo, T., and Sawayama, S. (2009). "Wet disk milling pretreatment without sulfuric acid for enzymatic hydrolysis of rice straw," *Bioresource Technol.* 100, 2706-2711. DOI: 10.1016/j.biortech.2008.12.057

Hideno, A. (2016). "Comparison of the thermal degradation properties of crystalline and amorphous cellulose, as well as treated lignocellulosic biomass," *BioResources* 11(3), 6309-6319. DOI: 10.15376/biores.11.3.6309-6319

Hideno, A., Abe, K., Uchimura, H., and Yano, H. (2016). "Preparation by combined enzymatic and mechanical treatment and characterization of nano fibrillated cotton fibers," *Cellulose* 23, 3639-3651. DOI: 10.1007/s10570-016-1075-y

Isogai, A., Saito, T., and Fukuzumi, H. (2011). "TEMPO-oxidized cellulose nanofibers," *Nanoscale* 3(1), 71-85. DOI: 10.1039/C0NR00583E

Kawamoto, H. (2015). "Reactions and molecular mechanisms of cellulose pyrolysis," *J. Jap. Wood Res. Soc.* 61(1), 1-24. DOI: 10.2488/jwrs.61.1

Kumagai, A., and Endo, T. (2018). "Comparison of the surface constitutions of hemicelluloses on lignocellulosic nanofibers prepared from softwood and hardwood," *Cellulose* 25, 3885-3897. DOI: 10.1007/s10570-018-1861-9

Quievy, N., Jacquet, N., Sclavons, M., Deroanne, C., Paquot, M., and Devaux, J. (2010). "Influence of homogenization and drying on the thermal stability of microfibrillated cellulose," *Poly. Deg. Stab.* 95(3), 306-314. DOI: 10.1016/j.polymdegradstab.2009.11.020

Segal, L., Creely, J. J., Martin, A. E., and Conrad, C. M. (1959). "An empirical method for estimating the degree of crystallinity of native cellulose using the X-ray diffractometer," *Text Res. J.* 29, 786-794. DOI: 10.1177/004051755902901003

Semba, T., Ito, A., Kitagawa, K., Kataoka, H., Nakatsubo, F., Kuboki, T., and Yano, H. (2021). "Polyamide 6 composites reinforced with nano fibrillated cellulose formed during compounding: Effect of acetyl group degree of substitution," *Composites Part A* 145, article 106385. DOI: 10.1016/j.compositesa.2021.106385

Sluiter, A., Hames, B., Scarlata, R.C., Sluiter, J., Templeton, D., and Crocker, D. (2008). *Determination of Structural Carbohydrates and Lignin in Biomass* (Technical Report NREL/TP-510-42618),

Wang, J., Minami, E., and Kawamoto, H. (2020). "Thermal reactivity of hemicellulose and cellulose in cedar and beech wood cell walls," *J. Wood Sci.* 66, 41. DOI: 10.1186/s10086-020-01888-x

Wang, J., Minami, E., Asmadi, M., and Kawamoto, H. (2021a). "Thermal degradation of hemicellulose and cellulose in ball-milled cedar and beech wood," *J. Wood Sci.* 67, 32. DOI: 10.1186/s10086-021-01962-y

Wang, J., Minami, E., Asmadi, M., and Kawamoto, H. (2021b). "Effect of delignification on thermal degradation reactivities of hemicellulose and cellulose in wood cell walls," *J. Wood Sci.* 67, 19. DOI: 10.1186/s10086-021-01952-0

Yano, H. (2010). "Production of cellulose nanofibers and their application," *Funct. Pap. Res. J.* 49, 15-20. DOI: 10.11332/kinoushi.49.15

Article submitted: September 27, 2023; Peer review completed: October 14, 2023;
Revised version received and accepted: October 18, 2023; Published: October 30, 2023.
DOI: 10.15376/biores.18.4.8573-8584